ФИЗИКА ЭЛЕМЕНТАРНЫХ ЧАСТИЦ И АТОМНОГО ЯДРА
2013. Т. 44. ВЫП. 3

TAMING LANDAU SINGULARITIES IN QCD PERTURBATION THEORY: THE ANALYTIC APPROACH 2.0*

*N. G. Stefanis***

Institut für Theoretische Physik II, Ruhr-Universität Bochum, Bochum, Germany

The aim of this topical article is to outline the fundamental ideas underlying the recently developed Fractional Analytic Perturbation Theory (FAPT) of QCD and to present its main calculational tools together with key applications. For this, it is first necessary to review previous methods to apply QCD perturbation theory at low spacelike momentum scales, where the influence of the Landau singularities becomes inevitable. Several concepts are considered and their limitations are pointed out. The usefulness of FAPT is discussed in terms of two characteristic hadronic quantities: the perturbatively calculable part of the pion's electromagnetic form factor in the spacelike region and the Higgs boson decay into a $b\bar{b}$ pair in the timelike region. In the first case, the focus is on the optimization of the prediction with respect to the choice of the renormalization scheme and the dependence on the renormalization and the factorization scales. The second case serves to show that the application of FAPT to this reaction reaches already at the four-loop level an accuracy of the order of 1%, avoiding difficulties inherent in the standard perturbative expansion. The obtained results are compared with estimates from fixed-order and contour-improved QCD perturbation theory. Using the brand-new Higgs mass value of about 125 GeV, measured at the Large Hadron Collider (CERN), a prediction for $\Gamma_{H\to b\bar{b}} = (2.4 \pm 0.15)$ MeV is extracted.

PACS: 11.10.Hi; 11.15.Bt; 12.38.Bx; 12.38.Cy; 13.40.Gp

INTRODUCTION

In writing this article, I have two main objectives. The first is to chart the evolution of the analytic approach to Quantum Chromodynamics (QCD) perturbation theory, focusing on the key turning points in its theoretical development. The second is to demonstrate how this approach works in terms of selected applications. Of course, I am forced to leave out many interesting applications and aspects of the approach, which in turn means that my presentation will not be complete. I would refer the reader to the original references for further reading

*This is an extended and updated version of an invited plenary talk at the International Conference «Renormalization Group and Related Topics» (RG 2008), Dubna, September 1–5, 2008.

**E-mail: stefanis@tp2.ruhr-uni-bochum.de

and in order to study the subject in more technical detail. The sorts of ideas and issues to be discussed in this presentation include the following benchmarks:

• «Ultraviolet (UV) freedom», «infrared (IR) slavery», and Landau singularity.

• Renormalizability, analyticity (in Q^2 and g^2), causality, and summability.

• First remedies in the infrared: color saturation, effective gluon mass.

• Screening of the Landau singularities via Sudakov form factors.

• Shirkov–Solovtsov analytic coupling — Euclidean and Minkowski spaces.

• From a recipe to a paradigm: Analytic Perturbation Theory (APT).

• More scales, more riddles: logarithms of the factorization (evolution) scale — naive and maximal analytization.

• Generalization of the analyticity requirement: from the coupling to the whole hadronic amplitude and its spectral density.

• Creation of Fractional APT (FAPT) in the spacelike and timelike regions.

• Summation of perturbation series, Sudakov gluon resummation (exponentiation vs. analytization), power corrections.

• Crossing of heavy-flavor thresholds.

The article is organized as follows. In Sec. 1, I review the two core characteristics of QCD: ultraviolet (UV) freedom and infrared (IR) confinement. The first attempts how to deal with the Landau singularity of the strong running coupling in the spacelike momentum region are described in Sec. 2. The analytization procedure of the coupling by Shirkov and Solovtsov is presented in Sec. 3, while its generalization to hadronic observables — in Sec. 4. Further extensions to accommodate more than one large scale are discussed in Sec. 5, followed in Sec. 6 by the analytization treatment of noninteger powers of the coupling that give rise to fractional analytic perturbation theory (FAPT) in the Euclidean and Minkowski space. Applications of FAPT are presented in Sec. 7 (pion's electromagnetic form factor) and in Sec. 8 (decay into a bottom–antibottom quark pair of a scalar Higgs boson).

1. ULTRAVIOLET FREEDOM AND INFRARED CONFINEMENT

Two key properties define QCD as the unbroken $SU(N_c = 3)$ (with N_c denoting the number of colors) Yang–Mills theory describing strong interactions at the microscopic level: asymptotic freedom and confinement. While the first property has been confirmed and was granted a Nobel prize in Physics in the year 2004, the other is still a matter of fact, with the underlying microscopic mechanism still at large. One claims that the reason for the nonobservation of free quarks and gluons in nature is due to their color content. From this, one concludes that only color singlets are observable — hence, de facto color confinement.

The main ingredient in justifying the UV freedom of QCD is that the renormalized QCD coupling becomes small at large momenta: $g^2 \to 0$ as $Q^2 \to \infty$ [1, 2]. This implies that though initially the coupling and the momentum scale are independent parameters*, they get linked to each other on account of the renormalizability of QCD. Hence, in the large-momentum region (or, equivalently, at short distances), QCD can be applied perturbatively, in analogy to QED in the sense of a weak-coupling expansion. A conventional way to define the running strong coupling in the $\overline{\rm MS}$ scheme is given by ($\alpha_s \equiv g^2/4\pi$)

$$\alpha_s(\mu) = \frac{12\pi}{(33-2N_f)\ln\left(\mu^2/\Lambda^2\right)}\left[1 - \frac{6(153-19N_f)}{(33-2N_f)^2}\,\frac{\ln\left[\ln\left(\mu^2/\Lambda^2\right)\right]}{\ln\left(\mu^2/\Lambda^2\right)}\right] + \\ + \mathcal{O}\left[\frac{1}{\ln^3(\mu^2/\Lambda^2)}\right], \quad (1)$$

which expresses it by means of the dimensional parameter $\Lambda \equiv \Lambda_{\rm QCD}$, whereas N_f represents the number of active flavors. For our considerations to follow it is more convenient to use the abbreviation $L \equiv \ln\left(\mu^2/\Lambda^2\right)$ and recast the above expression in terms of the first two coefficients of the β function

$$\mu^2\frac{d}{d\mu^2}\left(\frac{\alpha_s(\mu)}{4\pi}\right) = \beta\left(\frac{\alpha_s(\mu)}{4\pi}\right)\ , \quad (2)$$

namely,

$$b_0 = \frac{11}{3}C_A - \frac{4}{3}T_R N_f = 11 - \frac{2N_c}{3} \quad (3)$$

and

$$b_1 = \frac{34}{3}C_A^2 - \left(4C_F + \frac{20}{3}C_A\right)T_R N_f = 102 - \frac{38N_f}{3}, \quad (4)$$

where $C_F = (N_c^2-1)/2N_c = 4/3$, $C_A = N_c = 3$, and $T_R = 1/2$. Then, Eq. (1) becomes

$$\alpha_s[L(\mu)] = \frac{4\pi}{b_0}\,\frac{1}{L}\left[1 - \frac{b_1}{b_0^2}\,\frac{\ln[L]}{L}\right] + \mathcal{O}\left[\frac{1}{L^3}\right], \quad (5)$$

which is an approximate solution of the Renormalization-Group (RG) equation**

$$\frac{d}{dL}\left(\frac{\alpha_s(L)}{4\pi}\right) = -b_0\left(\frac{\alpha_s(L)}{4\pi}\right)^2 - b_1\left(\frac{\alpha_s(L)}{4\pi}\right)^3, \quad (6)$$

*Actually, there is no scale at all inside the QCD Lagrangian — provided one ignores current quark masses. A scale dependence is generated through dimensional transmutation.

**The first two coefficients β_0 and β_1 are scheme independent. The next coefficients β_2 and β_3 have also been analytically computed and confirmed by independent calculations at the level of 3 and 4 loops (see [3] for references).

exhibiting the asymptotic-freedom property, i.e., $\alpha_s \sim 1/\ln(\mu^2/\Lambda^2) \to 0$ as $\mu^2/\Lambda^2 \to \infty$. The scale parameter Λ is not a generic parameter of the QCD Lagrangian; its definition is arbitrary. However, once defined, it becomes the fundamental constant of QCD to be determined by experiment.

On the other hand, at $\mu^2 = \Lambda^2$ the running strong coupling has the Landau singularity that spoils analyticity. At the one-loop level this singularity is a simple pole, whereas at higher loops the corresponding Landau singularity has a more complicated structure (e.g., a square-root singularity at two loops, etc.). To restore analyticity in the infrared region $0 \leqslant Q^2 \leqslant \Lambda^2$ and ensure causality in the whole Q^2 plane, one has to remove the Landau singularity at any loop order of the perturbative expansion. This may become a serious problem, both theoretically and phenomenologically, for several hadronic processes — in particular, for exclusive processes like hadron form factors. For example, in the case of the spacelike pion's electromagnetic form factor — a typical exclusive process — most experimental data are available in a momentum region, where repercussions of the Landau singularity can influence (actually contaminate) the perturbative calculation, as is first shown and detailed in [4] and later further analyzed in [5]. Another way to describe this behavior is to use the language of information theory and consider a perturbatively calculable quantity, like the scaled pion factor vs. the momentum transfer Q^2, as being a *dynamic range* of quality of the perturbative expansion. In this context, the accuracy of the QCD perturbative result (*the signal*) depends on the magnitude of the running coupling. The larger Q^2, the smaller the coupling and, hence, the higher the precision of the (perturbative) calculation is. As one approaches the Landau singularity, the coupling increases rendering the perturbative expansion less and less precise, i.e., creating a kind of *noise*. When one reaches the Landau singularity, the «noise» (the uncertainty) becomes overwhelming and one is unable to extract any information (a clear «signal») from perturbation theory. The next few sections will show in more detail how this problem can be averted.

Of course, one may interpret the breakdown of perturbation theory at low momenta $\sim \Lambda$, as a «natural» consequence of the (unknown) confinement forces that prevail in this momentum region. The problem is that this breakdown is not universal but depends on the renormalization scheme adopted and the renormalization scale-fixing procedure used. For instance, adopting the Brodsky–Lepage–Mackenzie (BLM) commensurate-scale procedure, when including higher-order QCD perturbative corrections (see [4, 5] for further details), the BLM scale may become very low (compared to the original momentum scale) and deeply intruding into the «forbidden» nonperturbative region, where the running coupling blows up and perturbative QCD becomes invalid. An example: Using the BLM procedure in the calculation of the pion's electromagnetic form factor at NLO [5], the QCD running coupling may still «feel» the Landau singularity at momenta as large as 6 GeV^2, a region close to the largest momenta probed by experiment at

present for this reaction. Hence, the (scheme-dependent) optimization of the QCD perturbative expansion of typical hadronic quantities may depend in a crucial way on the IR behavior of the running coupling. It becomes clear that any attempt to apply an optimized renormalization prescription (and scheme) in high fixed-order perturbative calculations should make sure that the result is not distorted by artificial logarithmic enhancements originating from the Landau singularity. Clearing away this obstruction is a real challenge.

2. FIRST REMEDIES IN THE INFRARED

The simplest way to avoid the Landau singularity in Euclidean space is to use a rigid IR cutoff on its value, say, $\alpha_s^{\rm cutoff} \approx 0.5{-}0.7$, such as to render the perturbative expansion sound. A more sophisticated procedure is to assume that below some momentum scale $\mu_{\rm IR} \gtrsim \Lambda$ color forces saturate, so that quarks and gluons are confined within color-singlet states. The IR cutoff scale $\mu_{\rm IR}$ can be conceived of as an effective gluon mass m_g generated by the dynamics of confinement, as proposed by Cornwall (1982) [6] (for further references and applications, see [7]). This mechanism tames the Landau singularity, but the intrinsic scale m_g is an extraneous parameter to the approach and has to be determined by other methods, e.g., on the lattice [8]. Indeed, the saturated coupling at one loop reads

$$\alpha_s^{\rm sat}(Q^2) = \frac{4\pi}{\beta_0 \ln\left[(Q^2+\lambda^2)/\Lambda^2\right]} \tag{7}$$

with $\lambda^2 = 4m_g^2$ and is IR finite. Here m_g is a dynamical gluon mass with numerical values in the range (500 ± 200) MeV. This scale may be thought of as being the average transverse momentum of vacuum partons within the framework of nonlocal quark and gluon condensates. Technically, the role of the IR regulator m_g is to «freeze» $\alpha_s(Q^2)$ at low momenta $Q^2 \lesssim \lambda^2$, so that the coupling ceases to increase and flattens out.

An alternative approach to protect perturbatively calculated observables was developed by Sterman and collaborators [9, 10], in which α_s singularities were screened by Sudakov-type damping exponentials e^{-S} that encapsulate the effects of gluonic radiative corrections. These are resumed contributions stemming from two-particle reducible diagrams (giving rise to leading double logarithms), while two-particle irreducible diagrams (entailing subleading single logarithms) are absorbed into the hard-scattering part of the process. Because e^{-S} drops to zero faster than any power of $\ln(\mu^2/\Lambda^2_{\rm QCD})$, it provides sufficient IR protection against the Landau singularities both for mesonic amplitudes as well as for baryonic ones (see [7] for a review). Indeed, in the axial gauge, all Sudakov contributions due to unintegrated transverse momenta of the gluon propagators exponentiate

into suppressing Sudakov factors that suffice to render the Landau singularity of the one-loop running coupling in the form factors of the pion and the nucleon harmless, though the latter case is theoretically much more involved — see [7, 11, 12]. The main advantage of this approach relative to the previous one is that it contains an intrinsic IR regulator in terms of the impact parameter characterizing the interquark separations in the hadrons. Hence, there is no need for external IR regulators (like m_g) because IR protection is provided *in situ* by the Sudakov effect, the underlying idea being that gluons with wavelengths larger than the impact parameter «see» the quark configuration as a whole, i.e., in a color-singlet state and hence decouple. It is worth noting that the Sudakov suppression can be simulated by a saturated running coupling of the form of Eq. (7), if we assume that the IR cutoff parameter (i.e., the effective gluon mass) has to be adjusted to each individual value of the varying external momentum — for a mathematical version of this idea see [7]. Let us close this discussion by remarking that the application of this type of approach to the timelike region using analytic continuation is not straightforward owing to the fact that not only the running coupling has to be analytically continued but also the whole Sudakov form factor.

A bridge here is to what is to come in the next section with regard to analytization. In separate parallel developments, Krasnikov and Pivovarov (1982) [13], and independently Radyushkin (1982) [14], have obtained analytic expressions for the one-loop running coupling (and its powers) directly in Minkowski space using an integral transformation from the spacelike to the timelike region reverse to that for the Adler D-function. In both approaches a resummed Λ-parameterization for $\alpha_s(Q^2)$ in the spacelike region was employed in order to construct in the timelike region an expansion for $R(q^2)$ in which all $(\pi^2/L^2)^N$ terms ($L \equiv \ln s/\Lambda^2_{\rm QCD}$) are summed explicitly. This way, an analytic coupling in the timelike region was derived. This sort of analytic coupling in Minkowski space was rediscovered in the context of the resummation of fermion bubbles by Ball, Beneke, and Braun (1995) [15], partly in connection with techniques and applications to the τ hadronic width [16] (more references are given in [17]). Still other approaches to avoid ghost singularities in the running coupling are referenced in [4, 17].

3. INTO ANALYTIZATION

Shirkov and Solovtsov (1996) [18] have invented an analytic coupling based solely on Renormalization-Group (RG) invariance and causality (spectrality) in terms of a dispersion relation, generalizing the earlier work by Bogoliubov, Logunov, and Shirkov for QED [19]. The key ingredient of their framework is the spectral density $\rho_f(\sigma)$ with the aid of which an analytic running coupling can be

defined in the Euclidean region ($-q^2 = Q^2$) using a Källén–Lehmann spectral representation

$$[f(Q^2)]_{\rm an} = \int\limits_0^\infty \frac{\rho_f(\sigma)}{\sigma + Q^2 - i\epsilon}\, d\sigma. \tag{8}$$

The same spectral density $\rho_f(\sigma) = \mathrm{Im}\,[f(-\sigma)]/\pi$ is then used to define the running coupling also in the timelike region by means of a dispersion relation for the Adler function. At the one-loop level, one obtains for the image of $f(Q^2) = a(Q^2) \equiv (b_0/4\pi)\alpha_s(Q^2)$ in the Euclidean region [18]:

$$\mathcal{A}_1(Q^2) = \int\limits_0^\infty \frac{\rho(\sigma)}{\sigma + Q^2}\, d\sigma = \frac{1}{L} - \frac{1}{\mathrm{e}^L - 1}, \tag{9}$$

while its counterpart in Minkowski space reads

$$\mathfrak{A}_1(s) = \int\limits_s^\infty \frac{\rho(\sigma)}{\sigma}\, d\sigma = \frac{1}{\pi}\, \arccos \frac{L_s}{\sqrt{\pi^2 + L_s^2}}, \tag{10}$$

where $L = \ln\,(Q^2/\Lambda^2_{\rm QCD})$ and $L_s = \ln\,(s/\Lambda^2_{\rm QCD})$. Both couplings are analytic functions of their arguments. The analyticity of $\mathcal{A}_1(Q^2)$ is ensured by the second power-behaved term in (9) which removes the Landau (ghost) pole, whereas $\mathfrak{A}_1(s)$ does not contain any singular term at all. This analytization concept was used earlier in QED by Redmond and Uretsky (1958) [20] in connection with the elimination of ghosts in propagators, based on a term-by-term perturbation expansion in the coupling constant. The graphical representation of the removal of the Landau ghost in the coupling is shown in Fig. 1.

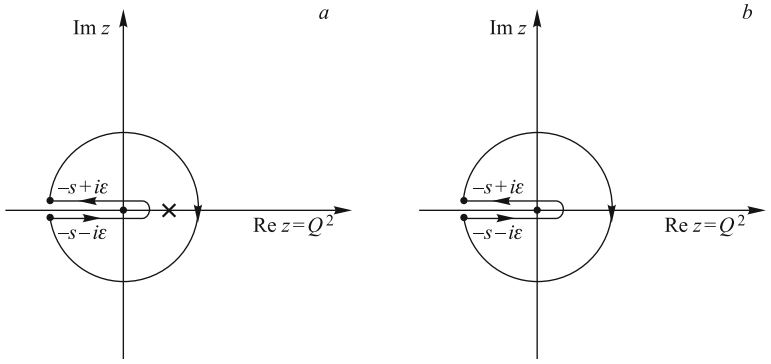

Fig. 1. The Landau singularity, marked by the symbol × in plot *a*, is absent by construction in the analytic approach of Shirkov and Solovtsov [18] (plot *b*)

4. THE BIRTH OF APT. FROM A CONCEPT TO A PARADIGM

The simple analytization concept for the one-loop running coupling in the spacelike region has been extended by its inventors and their collaborators to higher loops and has been applied to several characteristic hadronic processes. Examples are the inclusive decay of a τ lepton into hadrons, the momentum-scale and scheme dependence of the Bjorken and the Gross–Llewellyn Smith sum rule, Υ decays into hadrons, etc. (the corresponding references can be found in [17]). In Fig. 2, we show the first power (plot *a*) and the second power (plot *b*) of the analytic couplings in the Euclidean (calligraphic notation) and in the Minkowski (Gothic notation) spaces. All couplings are evaluated at the one-loop level. One appreciates from this figure that the spacelike and timelike analytic couplings have a distorted symmetry for finite values of their arguments, though asymptotically, i.e., for $L, L_s \to \infty$, they tend to the conventional coupling: $\mathcal{A}_n(L \to \infty) \Rightarrow \mathfrak{A}_n(L_s \to \infty) \Rightarrow a^n(L \to \infty)$ for $n \in \mathbb{N}$, bearing in mind that $a = (b_0/4\pi)\alpha_s$. As we will see later, this property is valid also for real indices $\nu \in \mathbb{R}$.

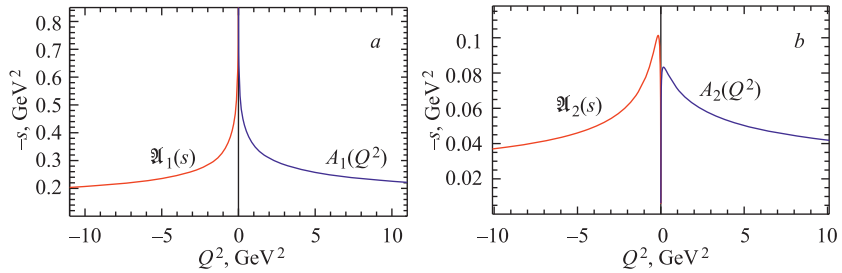

Fig. 2. Analytic couplings in APT: spacelike region — $\mathcal{A}_n(Q^2)$ and timelike region — $\mathfrak{A}_n(s)$. The plot *a* shows the first power (index), while the second power (index) is given in plot *b*

Meanwhile, a systematic approach — a new paradigm for perturbative calculations in QCD — has emerged, termed Analytic Perturbation Theory (APT). In a nutshell, it can be summarized as follows. The standard and the analytic couplings at one loop can be defined [17] recursively for any integer power (index) $n \in \mathbb{N}$ by means of

$$\begin{pmatrix} a^n(k) \\ \mathcal{A}_n(k) \\ \mathfrak{A}_n(k) \end{pmatrix} = \frac{1}{(n-1)!}\left(-\frac{d}{dk}\right)^{n-1} \begin{pmatrix} a^1(k) \\ \mathcal{A}_1(k) \\ \mathfrak{A}_1(k) \end{pmatrix}, \tag{11}$$

where a^n (standard QCD with the scaled coupling $a \equiv \alpha_s(b_0/4\pi) = 1/L$, $n \in \mathbb{N}$: power); $\mathcal{A}_n$ (analytic in spacelike region, $n \in \mathbb{N}$: index); $k = L \equiv \ln(Q^2/\Lambda^2)$; $\mathfrak{A}_n$ (analytic in timelike region, $n \in \mathbb{N}$: index); $k = L_s \equiv \ln(s/\Lambda^2)$.

On the other hand, in terms of the spectral density

$$\rho_n(\sigma) = \frac{1}{\pi}\,\mathrm{Im}\,[a^n(-\sigma)] = \frac{\sin\left[n\,\arccos\left(L_s/\sqrt{L_s^2+\pi^2}\right)\right]}{n\pi\left[\sqrt{L_s^2+\pi^2}\right]^n}, \tag{12}$$

one has

$$\mathcal{A}_n(Q^2) = \int\limits_0^\infty \frac{\rho_n(\sigma)}{\sigma+Q^2}d\sigma = \frac{1}{L^n} - \frac{F(e^{-L},1-n)}{\Gamma(n)}, \tag{13a}$$

$$\mathfrak{A}_n(s) = \int\limits_s^\infty \frac{\rho_n(\sigma)}{\sigma}\,d\sigma = \frac{\sin\left[(n-1)\,\arccos\left(L_s/\sqrt{L_s^2+\pi^2}\right)\right]}{(n-1)\pi\left[\sqrt{L_s^2+\pi^2}\right]^{n-1}}, \tag{13b}$$

where $F(z,n)$ is the transcendental Lerch function serving in (13a) as a Landau-pole remover [17]. In APT, hadronic quantities defined (in the Minkowski region) by $\oint f(z)R(z)\,dz$ with

$$R^{\mathrm{PT}}(z) = \sum_n r_m \alpha_s^m(z) \stackrel{\mathrm{APT}}{\longrightarrow} \mathcal{R}^{\mathrm{APT}}(z) = \sum_n d_m \mathfrak{A}_m(z) \tag{14}$$

have no Landau singularities in the Euclidean region, because the spacelike couplings $\mathcal{A}_n(z)$ are analytic functions. One appreciates that APT transforms a power-series expansion into a nonpower-series, i.e., a functional, expansion.

Let us close this section by making some important remarks (for references, see [17]):

— analytization in Euclidean space means subtraction of the Landau pole (at one loop);

— analytization in Minkowski space amounts to summation of π^2 terms;

— observables become nonpower-series expansions (i.e., n is an index not a power): $\mathcal{D}(Q^2) = \sum\limits_n d_n\,\mathcal{A}_n(Q^2)$ (Euclidean space), $\mathcal{R}(s) = \sum\limits_n d_n\,\mathfrak{A}_n(s)$ (Minkowski space);

— the elimination of ghost singularities in APT appears as a result of causality (spectrality) and RG invariance, i.e., the pole remover is not introduced by hand;

— two-loop expressions for the analytic couplings are possible by means of the Lambert function (Magradze (2000));

— still higher orders can be obtained with an approximate spectral density and employing numerical integration (Shirkov (1999));

— incorporation of heavy-quark flavors is possible («global APT» — Shirkov (2001));

— modifications of APT in the deep IR are possible via a spectral density which contains (nonperturbative) power corrections (Alekseev (2006); Nesterenko and Papavassiliou (2005); Cvetič and Valenzuela (2005)).

5. MORE SCALES, MORE RIDDLES

The above exposition suffices to demonstrate the usefulness of APT. But where are its limitations? Can the new paradigm be applied to more complicated cases that contain more than one large momentum scale? And can APT accommodate the crucial effect of evolution? As we cannot sidestep these problems, we will have to dig deeper into analytization. This is not a terminal difficulty of the analytic approach — and we can even benefit from it because doing so, we will ultimately expand APT to noninteger powers of the coupling. It is to these questions to which we focus now our attention.

To start with, we consider as a «theoretical laboratory» the factorized part of the spacelike pion's electromagnetic form factor. In NLO perturbation theory, this quantity can be written as a convolution $[A \otimes B \equiv \int\limits_0^1 dz A(z)B(z)]$ of a hard-scattering amplitude T and two pion distribution amplitudes, $\varphi_\pi^{\rm in}$, $\varphi_\pi^{\rm out}$, representing the incoming and outgoing pion bound states of quarks with longitudinal momentum fractions x and y, respectively. T is the amplitude for a collinear valence quark–antiquark pair, struck by a highly virtual photon with the large momentum Q^2, and contains hard-gluon exchanges characterized by the strong coupling α_s to the considered order of the expansion. Then, we have

$$F_\pi^{\rm fact}(Q^2) = \varphi_\pi^{\rm in}(x,\mu_F^2) \otimes T_H^{\rm NLO}\left(x,y,Q^2;\mu_F^2,\mu_R^2\right) \otimes \varphi_\pi^{\rm out}(y,\mu_F^2), \qquad (15)$$

where

$$\varphi_\pi(x,\mu^2) = 6x(1-x)\times \\ \times \left[1 + a_2(\mu^2)\, C_2^{3/2}(2x-1) + a_4(\mu^2)\, C_4^{3/2}(2x-1) + \ldots\right] \qquad (16)$$

is the leading twist-2 pion distribution amplitude containing the nonperturbative information on the pion quark structure in terms of the Gegenbauer coefficients a_n at the initial scale $\mu^2 \approx 1$ GeV^2, and T is the sum of all quark–gluon subprocesses up to the order α_s^2 (its explicit form can be found in the second paper in [4] and also in [5]). Note that T depends explicitly on α_s, whereas φ_π has a more complicated dependence controlled by the evolution equation. Besides, beyond the LO of perturbation theory, T depends not only on the large external momentum Q^2, but also on a second auxiliary momentum scale μ_F which separates the hard (perturbative) from the soft (nonperturbative) dynamics on account of a factorization theorem. Invariably, the soft parts, i.e., the pion distribution amplitudes, have to be evolved with appropriate anomalous dimensions from the initial scale μ^2 to the actual scale of observation Q^2. As we will discuss in the next section, this additional scale has influence on the analytization procedure that cannot be covered by APT.

The first application of APT to $F_\pi^{\rm fact}(Q^2)$ was considered in [4], in which the strong coupling and its powers were replaced by their corresponding analytic images: $a^n(L) \to (\mathcal{A}_1(L))^n$ (*Naive analytization* [5]). This treatment is, strictly speaking, incorrect because $[\mathcal{A}_1(L)]^n \neq [a_s^n(L)]_{\rm an}$, but phenomenologically it works rather good [4]. An improvement of this approach was presented in [5], where a *Maximal analytization* of this quantity was performed. This procedure associates to the powers of the running coupling their own dispersive images, i.e., $[a_s^n(L)]_{\text{max-an}} = \mathcal{A}_n(L)$. It is worth emphasizing that the analytization treatment was applied not only to the hard part T but also to the anomalous dimensions, governing the evolution of the pion distribution amplitudes, which can be computed order-by-order in perturbation theory. The differences between the two analytization procedures become apparent by comparing the following two expressions:

Naive analytization

$$\left[Q^2 T_H\left(x,y,Q^2;\mu_F^2,\lambda_R Q^2\right)\right]_{\text{naive-an}} = \mathcal{A}_1^{(2)}(\lambda_R Q^2)\, t_H^{(0)}(x,y) + \\ + \frac{[\mathcal{A}_1^{(2)}(\lambda_R Q^2)]^2}{4\pi}\, t_H^{(1)}\left(x,y;\lambda_R,\frac{\mu_F^2}{Q^2}\right), \quad (17)$$

Maximal analytization

$$\left[Q^2 T_H\left(x,y,Q^2;\mu_F^2,\lambda_R Q^2\right)\right]_{\text{max-an}} = \mathcal{A}_1^{(2)}(\lambda_R Q^2)\, t_H^{(0)}(x,y) + \\ + \frac{\mathcal{A}_2^{(2)}(\lambda_R Q^2)}{4\pi}\, t_H^{(1)}\left(x,y;\lambda_R,\frac{\mu_F^2}{Q^2}\right), \quad (18)$$

where $\lambda_R Q^2 = \mu_R^2$ serves as a renormalization scale, and μ_F^2 denotes the factorization scale of the process. The explicit form of the amplitudes $t_H^{(0)}$ and $t_H^{(1)}$ is irrelevant for our arguments here; it can be found in [4, 5, 21]. Furthermore, in [4], the (naive) analytization procedure was also applied after exponentiation to the Sudakov form factor in the next-to-leading logarithmic approximation of the cusp anomalous dimension.

Some technical comments: a) The pole remover in the one-loop running coupling does not change the leading double logarithmic behavior of the Sudakov factor, though the cusp anomalous dimension in the Sudakov exponent receives additional subleading contributions. b) Due to the absence of ghost singularities, the Sudakov exponents are analytic functions of Q^2. c) The perturbatively calculable part of the pion's electromagnetic form factor $Q^2 F_\pi^{\rm fact}(Q^2)$ receives the bulk of its contributions from small transverse distances b below $b\Lambda_{\rm QCD} \lesssim 0.5$, i.e., it saturates in exactly that region, where the application of QCD perturbation theory is valid [4]. However, the full treatment of the Sudakov-type gluon resummation in impact space faces special subtleties which have not been fully resolved until now. First results within a toy model in momentum space (see Appendix C

of [22]) seem to indicate a conflict between analytization and exponentiation of soft gluons.

Phenomenologically, already the «naive» analytization procedure and even more the «maximal» application of APT have important consequences: (i) the artificial increase of the spacelike electromagnetic pion form factor towards low Q^2 values — caused by the Landau singularity — is absent, (ii) the sensitivity of the results on the choice of the renormalization scheme and the adopted scale setting is extremely reduced relative to the standard power-series expansion of perturbative QCD (Shirkov and Solovtsov (1998) and [5]). This behavior is shown graphically in Fig. 3 for the scaled expression of $F_\pi^{\rm fact}(Q^2)$ employing these two analytization procedures and including leading-order evolution of the pion distribution amplitude in APT. The predictions shown were calculated for different renormalization-scale settings, including the «default» choice, $\mu_R^2 = Q^2$ (dashed line), the Brodsky–Lepage–Mackenzie scale setting (dotted line), the so-called $\alpha_{\rm V}$ scheme (dash-dotted line), etc., and employing the Bakulev–Mikhailov–Stefanis pion distribution amplitude which has $a_2(\mu_0^2 = 1\ \text{GeV}^2) = 0.20$, $a_4(\mu_0^2 = 1\ \text{GeV}^2) = -0.14$, $a_n(\mu_0^2 = 1\ \text{GeV}^2) \approx 0$ $(n > 2)$. All these issues are discussed in detail in [5]. The main observation from this figure is that applying APT in its maximal form to a typical exclusive quantity, like $F_\pi^{\rm fact}(Q^2)$, not only provides IR stability, it also diminishes its renormalization scheme and scale-setting dependence already at the NLO level. Indeed, the predictions obtained in different schemes do not differ significantly from each other in a wide range of momenta from low to large Q^2 values.

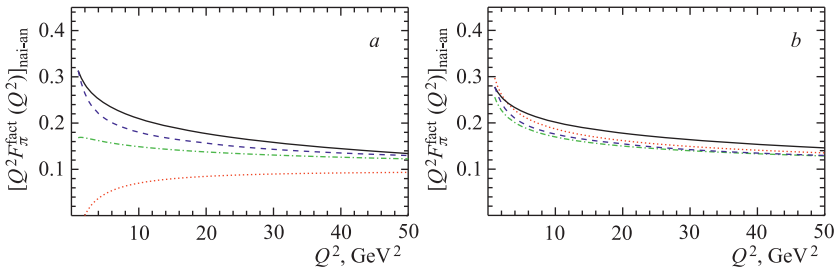

Fig. 3. Results for $Q^2 F_\pi^{\rm fact}(Q^2)$ vs. Q^2 with $\mu_R^2 = Q^2$, $\mu_F^2 = 5.76\ \text{GeV}^2$ and using Naive analytization (*a*) and with Maximal analytization (*b*) for various renormalization-scale settings described in [5]. All predictions have been calculated with the Bakulev–Mikhailov–Stefanis pion distribution amplitude (see [5] for references)

To further appreciate the advantages of the analytic scheme relative to the standard power-series expansion, bear in mind our statements in Sec. 1 in the language of information theory. Within this context, one may consider the variation of the predictions — the uncertainty spread — obtained with different renormal-

ization schemes, as «noise», the prediction for $F_\pi^{\rm fact}(Q^2)$ itself being the «signal». It becomes obvious from Fig. 3, *b* that maximal analytization within APT provides a much better dynamical range of quality because the signal-to-noise ratio is strongly enhanced in the whole Q^2 range, especially at low Q^2.

6. FRACTIONALIZING APT

In the previous section, we have discussed the advantages of APT relative to the standard QCD perturbation theory and considered a typical exclusive quantity, notably, the factorizable part of the pion's electromagnetic form factor that exhibits a dependence on potentially two large momentum scales: Q^2 and the factorization scale μ_F (that may also serve as the evolution parameter). Until now our discussion has not addressed the factorization-scale dependence under the proviso of analytization. But the considered example makes it obvious that, ultimately, one has to accommodate the analytization of terms like

$$\begin{aligned} &Z[L] = \exp\left[\int^{a_s[L]} \frac{\gamma(a)}{\beta(a)} da\right] \to [a_s(L)]^{\gamma_0/2\beta_0} \longleftrightarrow \text{RG at one loop},\\ &[a_s(L)]^n \ln[a_s(L)] \longleftrightarrow \text{RG at two loops},\\ &[a_s(L)]^n L^m \longleftrightarrow \text{factorization},\\ &\exp[-a_s(L)F(x)] \longleftrightarrow \text{Sudakov resummation} \end{aligned} \tag{19}$$

typically appearing in perturbative calculations beyond LO, as in our example. Though such terms do not modify ghost singularities, say, the position of the Landau pole in the one-loop approximation, they do contribute to the spectral density. To include such terms into the dispersion integral, one is actually forced to modify the analyticity requirement and demand not only the analyticity of the running coupling and its powers, but rather the analyticity of the quark–gluon amplitude as a whole [23]. This generalized encompassing version of the analyticity requirement demands that all terms that may contribute to the spectral density, i.e., affect the discontinuity across the cut along the negative real axis $-\infty < Q^2 < 0$, must be included into the analytization procedure [21–23]. The use of this principle allows the inclusion into the dispersion relation of logarithmic terms of the sort $\ln(Q^2/\mu_F^2)$, or products of such logarithms containing powers of the running coupling. It turns out that precisely such terms are tantamount to *fractional* (in fact, real) powers of the strong coupling, pertaining to FAPT [17, 22].

Before studying the consequences of this generalized analyticity requirement for observables, let us first present the different analytization concepts, we have

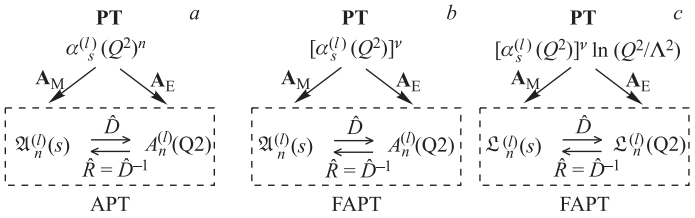

Fig. 4. Implementation of analyticity in standard QCD perturbation theory (PT), APT (*a*), and in FAPT (*b*, *c*)

discussed above, in mutual comparison (Fig. 4). In this figure, the linear operations $\mathbf{A}_\mathrm{E}$ and $\mathbf{A}_\mathrm{M}$ define, respectively, the analytic running couplings in the Euclidean (spacelike)

$$\mathbf{A}_\mathrm{E}\left[a_{(l)}^n\right] = \mathcal{A}_n^{(l)} \quad \text{with} \quad \mathcal{A}_n^{(l)}(Q^2) \equiv \int\limits_0^\infty \frac{\rho_n^{(l)}(\sigma)}{\sigma + Q^2}\, d\sigma \tag{20}$$

and the Minkowski (timelike) region

$$\mathbf{A}_\mathrm{M}\left[a_{(l)}^n\right] = \mathfrak{A}_n^{(l)} \quad \text{with} \quad \mathfrak{A}_n^{(l)}(s) \equiv \int\limits_s^\infty \frac{\rho_n^{(l)}(\sigma)}{\sigma}\, d\sigma, \tag{21}$$

where the loop order of the expansion is denoted by the superscript (l). The above analytization operations can be represented by the following two integral transformations from the timelike region to the spacelike one:

$$\hat{D}\left[\mathfrak{A}_n^{(l)}\right] = \mathcal{A}_n^{(l)} \quad \text{with} \quad \mathcal{A}_n^{(l)}(Q^2) \equiv Q^2 \int\limits_0^\infty \frac{\mathfrak{A}_n^{(l)}(\sigma)}{\left(\sigma + Q^2\right)^2}\, d\sigma \tag{22}$$

and for the inverse transformation

$$\hat{R}\left[\mathcal{A}_n^{(l)}\right] = \mathfrak{A}_n^{(l)} \quad \text{with} \quad \mathfrak{A}_n^{(l)}(s) \equiv \frac{1}{2\pi i} \int\limits_{-s-i\varepsilon}^{-s+i\varepsilon} \frac{\mathcal{A}_n^{(l)}(\sigma)}{\sigma}\, d\sigma. \tag{23}$$

These two integral transformations are interrelated:

$$\hat{D}\hat{R} = \hat{R}\hat{D} = 1 \tag{24}$$

for the whole set of analytic images of the powers of the coupling in the Euclidean, as well as in the Minkowski space, $\left\{\mathcal{A}_n, \mathfrak{A}_n\right\}$, respectively, and at any desired

loop order of the perturbative expansion. Then, Eq. (13a) generalizes from integer indices n to any real index $\nu \in \mathbb{R}$ to read (Euclidean space)

$$\mathcal{A}_\nu(L) = \frac{1}{L^\nu} - \frac{F(\mathrm{e}^{-L}, 1-\nu)}{\Gamma(\nu)}, \tag{25}$$

where the first term corresponds to the conventional term of perturbative QCD (with $L \equiv \ln(Q^2/\Lambda^2)$) and the second one is entailed by the pole remover (cf. $1/(\mathrm{e}^L - 1)$ at one loop). The function $\mathcal{A}_\nu(L)$ is an entire function in the index ν and has the following properties:

— $\mathcal{A}_0(L) = 1$;

— $\mathcal{A}_{-m}(L) = L^m = a^{-m}(L)$ for $m \in \mathbb{N}$. Hence, the inverse powers of the analytic coupling and the original running coupling coincide);

— $\mathcal{A}_m(\pm\infty) = 0$ for $m \geqslant 2$, $m \in \mathbb{N}$;

— $\mathcal{A}_\nu(L) = -[1/\Gamma(\nu)] \sum\limits_{r=0}^{\infty} \zeta(1-\nu-r)[(-L)^r/r!]$ for $|L| < 2\pi$.

Note that the reduced transcendental Lerch function $F(z,\nu)$ is related to the Lerch function $\Phi(z,\nu,m)$ via $z\Phi(z,\nu,1) \equiv F(z,\nu)$. For a positive integer index, $\nu = m \geqslant 2$, one has the relation

$$F(z, 1-m) = (-1)^m F\left(\frac{1}{z}, 1-m\right), \tag{26}$$

so that substituting Eq. (26) into (25), one arrives at

$$\mathcal{A}_m(L) = (-1)^m \mathcal{A}_m(-L). \tag{27}$$

In Minkowski space, the analytic images of the running coupling are completely determined by elementary functions [22] ($L_s \equiv \ln(s/\Lambda^2)$):

$$\mathfrak{A}_\nu(L_s) = \frac{\sin\left[(\nu-1)\arccos\left(L_s/\sqrt{\pi^2+L_s^2}\right)\right]}{\pi(\nu-1)(\pi^2+L_s^2)^{(\nu-1)/2}} \tag{28}$$

from which, for example, we get $\mathfrak{A}_0(L_s) = 1$, $\mathfrak{A}_{-1}(L_s) = L_s$; $\mathfrak{A}_{-2}(L) = L^2 - \pi^2/3$; $\mathfrak{A}_m(L) = (-1)^m \mathfrak{A}_m(-L)$ for $m \geqslant 2$; $\mathfrak{A}_m(-\infty) = \mathcal{A}_m(-\infty) = \delta_{m,1}$; $\mathfrak{A}_m(\infty) = \mathcal{A}_m(\infty) = 0$ for $m \in \mathbb{N}$. For the value $L = L_s = 0$, the analytic couplings in both regions are interrelated by the equation

$$\mathcal{A}_\nu(0) = \left[\frac{(\nu-1)\,\zeta(\nu)}{2^{\,\nu-1}}\right] \mathfrak{A}_\nu(0), \tag{29}$$

where

$$\mathfrak{A}_\nu(0) = \frac{\sin\left[(\nu-1)\pi/2\right]}{(\nu-1)\,\pi^\nu}, \tag{30}$$

and where $\zeta(\nu)$ is the Riemann ζ function, with the coefficient in the brackets providing a quantitative measure for the magnitude of the distortion of the «mirror symmetry», mentioned before, for any $\nu \in \mathbb{R}$. A graphical illustration of the analytic couplings $\mathcal{A}_\nu$ and $\mathfrak{A}_\nu$ is given in Fig. 5 which shows the rate of change of these functions with respect to the index ν and the argument L (or L_s).

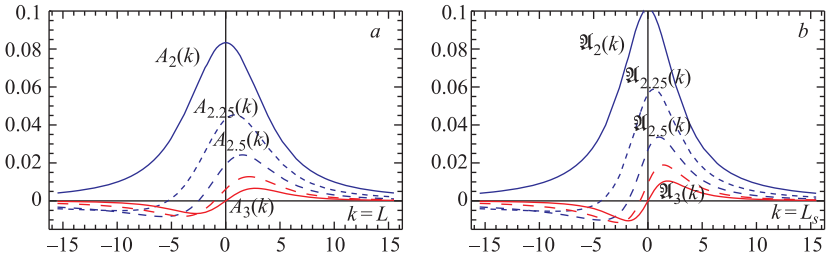

Fig. 5. Comparison of the Euclidean (a) and the Minkowski (b) analytic couplings, $\mathcal{A}_\nu(k=L)$ and $\mathfrak{A}_\nu(k=L_s)$, respectively, for incremental changes of the index ν in the range 2 to 3

Table 1. **FAPT versus standard QCD perturbation theory (SPT) and APT**

Theory	SPT	APT	FAPT
Space	$\{a^\nu\}_{\nu\in\mathbb{R}}$	$\{\mathcal{A}_m,\ \mathfrak{A}_m\}_{m\in\mathbb{N}}$	$\{\mathcal{A}_\nu,\ \mathfrak{A}_\nu\}_{\nu\in\mathbb{R}}$
Series expansion	$\sum\limits_m f_m\, a^m(L)$	$\sum\limits_m f_m\, \mathcal{A}_m(L)$	$\sum\limits_m f_m\, \mathcal{A}_m(L)$
Inverse powers	$[a(L)]^{-m}$	—	$\mathcal{A}_{-m}(L) = L^m$
Multiplication	$a^\mu a^\nu = a^{\mu+\nu}$	—	—
Index derivative	$a^\nu \ln^k a$	—	$\dfrac{d^k}{d\nu^k}\begin{pmatrix}\mathcal{A}_\nu\\ \mathfrak{A}_\nu\end{pmatrix} = [a^\nu \ln^k(a)]_{\rm an}$

The major characteristics of FAPT in comparison with the standard perturbative expansion in QCD and the original APT are collected in Table 1, while further details can be found in [17, 21, 22].

Up to now we have actually concentrated our attention on the one-loop approximation of the running coupling and its analytic images. But the index derivative in FAPT gives us the possibility to obtain two-loop expressions from those at one loop. To achieve this goal, let us recall the two-loop RG equation for the standard QCD normalized coupling $a_{(2)} = b_0\alpha_s^{(2)}/4\pi$

$$\frac{da_{(2)}(L)}{dL} = -a_{(2)}^2(L)\left[1 + c_1\, a_{(2)}(L)\right] \quad \text{with} \quad c_1 \equiv \frac{b_1}{b_0^2}, \tag{31}$$

which assumes the following functional form:

$$\frac{1}{a_{(2)}} + c_1 \ln\left[\frac{a_{(2)}}{1 + c_1 a_{(2)}}\right] = L. \tag{32}$$

This equation has the following exact solution (Magradze (2000)):

$$a_{(2)}(L) = -\frac{1}{c_1}\frac{1}{1 + W_{-1}(z_W(L))}, \tag{33}$$

where $z_W(L) = (1/c_1)\exp\,(-1 + i\pi - L/c_1)$ with W_k $(k = 0, \pm 1, \ldots)$ being the Lambert function, defined by $z = W(z)\exp\,(W(z))$, where its different branches are depicted by the index k.

With the above expression in our hands, we can immediately obtain [22] the spectral density at the two-loop level, $\rho_\nu^{(2)}(\sigma)$, by virtue of Eq. (12), viz.,

$$\rho_\nu^{(2)}(\sigma) = \frac{1}{\pi}\,\mathrm{Im}\,[a_{(2)}^\nu(L - i\pi)]. \tag{34}$$

Using this expression in Eqs. (20) and (21), we have

$$\mathcal{A}_\nu^{(2)}(L) = \int_0^\infty \frac{\rho_\nu^{(2)}(\sigma)}{\sigma + Q^2}\,d\sigma, \quad \mathfrak{A}_\nu^{(2)}(s) = \int_s^\infty \frac{\rho_\nu^{(2)}(\sigma)}{\sigma}\,d\sigma \tag{35}$$

from which we derive $(\mathcal{D} \equiv d^k/d\nu^k)$

$$\mathcal{A}_1^{(2)}(L) = \mathcal{A}_1^{(1)} + c_1\,\mathcal{D}\,\mathcal{A}_{\nu=2}^{(1)} + c_1^2(\mathcal{D}^2 + \mathcal{D} - 1)\mathcal{A}_{\nu=3}^{(1)} + \mathcal{O}(\mathcal{D}^3\,\mathcal{A}_{\nu=4}^{(1)}), \tag{36}$$

where we have expanded $a_{(2)}(L)$ in terms of $a_{(1)}(L)$. The above expression can be generalized to any real index ν, in both the Euclidean and the Minkowski spaces, to obtain

$$\begin{pmatrix}\mathcal{A}_\nu^{(2)}\\ \mathfrak{A}_\nu^{(2)}\end{pmatrix} = \begin{pmatrix}\mathcal{A}_\nu^{(1)}\\ \mathfrak{A}_\nu^{(1)}\end{pmatrix} + c_1\,\nu\,\mathcal{D}\begin{pmatrix}\mathcal{A}_{\nu+1}^{(1)}\\ \mathfrak{A}_{\nu+1}^{(1)}\end{pmatrix} + \\ + c_1^2\,\nu\left[\frac{\nu+1}{2!}\,\mathcal{D}^2 + \mathcal{D} - 1\right]\begin{pmatrix}\mathcal{A}_{\nu+2}^{(1)}\\ \mathfrak{A}_{\nu+2}^{(1)}\end{pmatrix} + \mathcal{O}(c_1^3). \tag{37}$$

Though these expressions are not exact, the achieved accuracy is of the order of about 1% down to the value $L = L_s = 0$ and, hence, they are sufficient for most practical QCD applications. A more accurate expression for the two-loop Minkowski coupling which includes the contribution of the next higher order $\mathcal{O}(\mathcal{D}^4\,\mathfrak{A}_{\nu+4}^{(1)})$ is given in [17]. Moreover, one can find there the analogous three-loop expression with a similarly good quality of convergence.

The particular advantage of FAPT is the possibility of performing the analytization of powers of the running coupling multiplied by logarithms of L and its powers, e.g., $[(a_{(2)}(L))^\nu L^m]_{\rm an} \equiv \mathcal{L}^{(2)}_{\nu,m}(L)$. As we emphasized before, such terms appear already in NLO calculations of typical hadronic amplitudes, like form factors, or when taking into account evolution effects. Table 2 displays in approximate form the analytization of such expressions. Their usefulness will become evident below, when we will consider the influence of such terms in the calculation of the factorized part of the pion's electromagnetic form factor.

Table 2. **Calculational rules for FAPT with $L = \ln\left(Q^2/\Lambda^2\right)$, $m \in \mathbb{N}$, and $\nu \in \mathbb{R}$. J_1 is a Bessel function of the first kind and $\psi(z) = d\ln\Gamma(z)/dz$ denotes the digamma function**

Standard QCD PT	QCD FAPT
$a^\nu_{(1)}(L) = \dfrac{1}{L^\nu}$	$\mathcal{A}^{(1)}_\nu(L) = \dfrac{1}{L^\nu} - \dfrac{F(e^{-L}, 1-\nu)}{\Gamma(\nu)}$
$a^\nu_{(l)}(L)\ \ln^m[a_{(l)}(L)]$	$\mathcal{D}^m\,\mathcal{A}^{(l)}_\nu(L) \equiv \dfrac{d^m}{d\nu^m}[\mathcal{A}^{(l)}_\nu(L)]$
$a^\nu_{(2)}(L)$	$\mathcal{A}^{(2)}_\nu(L) = \mathcal{A}^{(1)}_\nu(L) + c_1\nu\mathcal{D}\mathcal{A}^{(1)}_{\nu+1}(L) +$ $+c_1^2\nu\left[\dfrac{(\nu+1)}{2}\mathcal{D}^2 + \mathcal{D} - 1\right]\mathcal{A}^{(1)}_{\nu+2}(L) + \mathcal{O}(\mathcal{D}^3\mathcal{A}^{(1)}_{\nu+3})$
$a^\nu_{(2)}(L)\,L$	$\mathcal{L}^{(2)}_{\nu,1}(L) = \mathcal{A}^{(2)}_{\nu-1}(L) + c_1\mathcal{D}\mathcal{A}^{(2)}_\nu(L) + \mathcal{O}(\mathcal{D}^2\mathcal{A}^{(2)}_{\nu+1}) \approx \mathcal{A}^{(1)}_{\nu-1}(L) -$ $-c_1\nu\left[\dfrac{\ln(L) - \psi(\nu)}{L^\nu} + \psi(\nu)\mathcal{A}^{(1)}_\nu(L) + \dfrac{\mathcal{D}F(\mathrm{e}^{-L}, 1-\nu)}{\Gamma(\nu)}\right]$
$a^\nu_{(2)}(L)\,L^2$	$\mathcal{L}^{(2)}_{\nu,2}(L) = \mathcal{A}^{(2)}_{\nu-2}(L) + 2c_1\mathcal{D}\mathcal{A}^{(2)}_{\nu-1}(L) + c_1^2\mathcal{D}^2\mathcal{A}^{(2)}_\nu(L) -$ $-2c_1^2\,\mathcal{A}^{(2)}_\nu(L) + \mathcal{O}(\mathcal{D}\,\mathcal{A}^{(2)}_{\nu+1}) \approx \mathcal{A}^{(1)}_{\nu-2}(L) + c_1\nu\mathcal{D}\mathcal{A}^{(1)}_{\nu-1}(L) +$ $+c_1^2\left[\dfrac{\nu^2-\nu+4}{2}\right]\mathcal{D}^2\mathcal{A}^{(1)}_\nu(L)$
$\exp\left[-xa(L)\right]$	$\mathrm{e}^{-x/L} + \sqrt{x}\sum\limits_{m=1}\mathrm{e}^{-mL}\dfrac{J_1(2\sqrt{xm})}{\sqrt{m}}$ for $L > 0$

7. SPACELIKE PION'S ELECTROMAGNETIC FORM FACTOR IN FAPT

Having set up the calculational tools of FAPT, we now detail concrete applications, starting with an example in the spacelike region. Consider again Eq. (18) — this time including into the analytization procedure also the logarithmic term (labeled by the acronym KS [23] in order to indicate the analytization of the amplitude as a whole): $\ln(Q^2/\mu_F^2) = \ln(\lambda_R Q^2/\Lambda^2) - \ln(\lambda_R\mu_F^2/\Lambda^2)$. Then,

we find ($\bar{x} = 1 - x$)

$$\left[Q^2 T_H(x,y,Q^2;\mu_F^2,\lambda_R Q^2)\right]^{\rm an}_{\rm KS} = \\ = \mathcal{A}_1^{(2)}(\lambda_R Q^2)\, t_H^{(0)}(x,y) + \frac{\mathcal{A}_2^{(2)}(\lambda_R Q^2)}{4\pi}\, t_H^{(1)}\left(x,y;\lambda_R,\frac{\mu_F^2}{Q^2}\right) + \\ + \frac{\Delta_2^{(2)}(\lambda_R Q^2)}{4\pi}\left[C_F t_H^{(0)}(x,y)(6+2\ln(\bar{x}\bar{y}))\right], \quad (38)$$

with

$$\Delta_2^{(2)}(Q^2) \equiv \mathcal{L}_2^{(2)}(Q^2) - \mathcal{A}_2^{(2)}(Q^2)\,\ln[Q^2/\Lambda^2] \quad (39)$$

encoding the deviation from the result obtained with the Maximal analytization procedure and where

$$\mathcal{L}_2^{(2)}(Q^2) \equiv \left[(\alpha_s^{(2)}(Q^2))^2 \ln\left(\frac{Q^2}{\Lambda^2}\right)\right]^{\rm an}_{\rm KS} = \frac{4\pi}{b_0}\left[\frac{(\alpha_s^{(2)}(Q^2))^2}{\alpha_s^{(1)}(Q^2)}\right]^{\rm an}_{\rm KS}. \quad (40)$$

Carrying out the KS analytization, we get the approximate expression

$$\mathcal{L}_{2,1}^{{\rm appr}(2)}(Q^2) = \frac{4\pi}{b_0}\left[\mathcal{A}_1^{(2)}(Q^2) + c_1\,\frac{4\pi}{b_0}\, f_{\mathcal{L}}(Q^2)\right] \quad (41)$$

(which can be further improved by substituting the c_1-term in Eq. (41) by its two-loop expression: $\mathcal{L}_{2,1}^{{\rm imp};(2)}[L] = \mathcal{A}_1^{(2)}[L] + c_1 \mathcal{D}\mathcal{A}_2^{(2)}[L]$, see [24]), where (cf. Table 2, $a_{(2)}^{\nu=2}(L)L$)

$$f_{\mathcal{L}}(Q^2) = \sum_{n\geqslant 0}\left[\psi(2)\zeta(-n-1) - \frac{d\zeta(-n-1)}{dn}\right]\frac{\left[-\ln\left(Q^2/\Lambda^2\right)\right]^n}{\Gamma(n+1)} \quad (42)$$

and $\zeta(z)$ is the Riemann zeta function. The main effect of including the logarithmic term into the analytization procedure of $F_\pi^{\rm fact}(Q^2)$ is to suppress its sensitivity on the variation of the factorization scale to a minimum. It was shown in [21] that varying the factorization scale from 1 to 10 GeV^2, the form factor changes by a mere 1.5% reaching for a (hypothetical) factorization scale of 50 GeV^2 just the level of about 2.5%. Note here that it is possible to treat this problem in another way, namely, to fix $\mu^2 = Q^2$ from the very beginning and then use FAPT to correctly account for the evolution factors $E_n^{\rm LO}(Q^2) \sim \alpha_s^{\nu_n}(Q^2)$ in the Gegenbauer coefficients $a_n(Q^2)$, with ν_n being the corresponding fractional evolution exponents. This type of calculation was performed in [24] and it was shown that the difference between the two approaches, i.e., FAPT with fixed $\mu^2 = 5.76$ GeV^2 and FAPT with the renormalization scale fixed at $\mu^2 = Q^2$, is of the order of 1.5%.

To conclude, using FAPT, the dependence of a perturbatively calculated QCD quantity on all perturbative scheme and scale settings is diminished already at the NLO level.

8. HIGGS BOSON DECAY INTO A $b\bar{b}$ PAIR USING FAPT IN MINKOWSKI SPACE

The second FAPT application deals with the Higgs boson decay into a $b\bar{b}$ pair in the timelike region. We will present here only the main results and refer for the technical details to [17,25]. A dedicated analysis of the uncertainties involved in the calculation of the decay width of the Higgs boson into bottom quarks was recently given by Kataev and Kim [3].

Consider now the decay of a scalar Higgs boson to a $b\bar{b}$ pair in terms of the quantity R_S at the four-loop level from which one can then obtain the width $\Gamma(H \to b\bar{b})$. Note that the application of FAPT in Minkowski space is not plagued by Landau singularities. However, the analytic continuation from the spacelike to the timelike region induces the so-called «kinematical» π^2 terms that may be comparable in magnitude with the higher-order expansion coefficients and have, therefore, to be summed. The first step in our approach is the correlator of two scalar currents $J_b^S = \bar{\Psi}_b \Psi_b$ for bottom quarks with mass m_b, coupled to the scalar Higgs boson with mass M_H, and where $Q^2 = -q^2$, i.e.,

$$\Pi(Q^2) = (4\pi)^2 i \int dx \, \mathrm{e}^{iq\cdot x} \langle 0| \, T[J_b^S(x) J_b^S(0)] \, |0\rangle. \tag{43}$$

Then, $R_S(s) = \operatorname{Im}\Pi(-s - i\epsilon)/(2\pi s)$ and one can express the decay width in terms of R_S:

$$\Gamma(\mathrm{H} \to b\bar{b}) = \frac{G_F}{4\sqrt{2}\pi} M_H m_b^2(M_H) R_S(s = M_H^2). \tag{44}$$

The quantity R_S is obtained from the Adler function D via analytic continuation into the Euclidean space using the transformation $\mathbf{A}_M$ (or, equivalently, the integral transformation $\hat{R}$), as shown in Fig. 4. The reason for this detour is that in the Euclidean region perturbation theory works. Hence, we write

$$\widetilde{D}_{\mathrm{S}}(Q^2;\mu^2) = 3\, m_b^2(Q^2) \left[1 + \sum_{n\geqslant 1} d_n \left(\frac{Q^2}{\mu^2}\right) \, a_s^n(\mu^2)\right]. \tag{45}$$

The second step is to calculate

$$\widetilde{R}_{\mathrm{S}}(s) \equiv \widetilde{R}_{\mathrm{S}}(Q^2 = s, \mu^2 = s) = 3 m_b^2(s) \left[1 + \sum_{n\geqslant 1} r_n \, a_s^n(s)\right] \tag{46}$$

using the techniques developed by Gorishnii et al. (1990) [26] and Chetyrkin et al. (1997) [27].

As already mentioned, the coefficients r_n contain characteristic π^2 terms originating from the integral transformation $\hat{R}$ of the powers of the logarithms entering $\widetilde{D}_S$. The latter is related to $\widetilde{R}_S(s,s)$ by means of a dispersion relation. Notice that these logarithms have two different sources: one is the running of a_s in $\widetilde{D}_S$, while the other is related to the evolution of the heavy-quark mass $m_b^2(Q^2)$. As a result, the coefficients r_n in (46) are connected to the coefficients d_n in $\widetilde{D}_S$ (calculable in Euclidean space) and to a combination of the mass anomalous dimension γ_i and the β-function coefficients b_j multiplied by π^2 powers. Appealing to the explicit results given in [17], we remark that the total amount of these terms is of the order of the coefficient d_4. FAPT can, by construction, account for these terms to all orders of the perturbative expansion. This is because in FAPT one does not need to expand the renormalization factors into a truncated series of logarithms; instead one can transform them by means of the $\mathbf{A}_M$-operation «as a whole».

The running mass in the l-loop approximation, $m_{(l)}$, can be cast in terms of the renormalization-group invariant quantity $\hat{m}_{(l)}$ to read

$$m^2_{(l)}(Q^2) = \hat{m}^2_{(l)}[a_s(Q^2)]^{\nu_0} f_{(l)}(a_s(Q^2)), \tag{47}$$

where $\nu_0 = 2\gamma_0/b_0$ and the expansion of $f_{(l)}(x)$ at the three-loop order is given by

$$\begin{aligned} f_{(l)}(a_s) = 1 + a_s \frac{b_1}{2b_0}\left(\frac{\gamma_1}{b_1} - \frac{\gamma_0}{b_0}\right) + \\ + a_s^2 \frac{b_1^2}{16\, b_0^2}\left[\frac{\gamma_0}{b_0} - \frac{\gamma_1}{b_1} + 2\left(\frac{\gamma_0}{b_0} - \frac{\gamma_1}{b_1}\right)^2 - \right. \\ \left. + \frac{b_0 b_2}{b_1^2}\left(\frac{\gamma_2}{b_2} - \frac{\gamma_0}{b_0}\right)\right] + O\left(a_s^3\right). \end{aligned} \tag{48}$$

Expanding the running mass in a power series according to

$$m^2_{(l)}(Q^2) = \hat{m}^2_{(l)}\,(a_s(Q^2))^{\nu_0}\left[1 + \sum_{m\geqslant 1}^{\infty} e^{(l)}_m (a_s(Q^2))^m\right], \tag{49}$$

and setting $\mu^2 = Q^2$, we find

$$\begin{aligned} [3\,\hat{m}_b^2]^{-1}_{(l)}\,\widetilde{D}^{(l)}_S(Q^2) = (a_s^{(l)}(Q^2))^{\nu_0} + \\ + \sum_{n\geqslant 1}^{l} d_n\,(a_s^{(l)}(Q^2))^{n+\nu_0} + \sum_{m\geqslant 1}^{\infty} \Delta^{(l)}_m\,(a_s^{(l)}(Q^2))^{m+\nu_0} \end{aligned} \tag{50}$$

with

$$\Delta_m^{(l)} = e_m^{(l)} + \sum_{k\geqslant 1}^{\min[l,m-1]} d_k\, e_{m-k}^{(l)}. \tag{51}$$

Note that we have separated the mass-evolution multiloop effects (third term of Eq. (50)) from the original series expansion of D (truncated at $n = l$). These contributions are represented by the second term on the RHS of Eq. (50). In practice, for $Q \geqslant 2$ GeV, i.e., for $\alpha_s \leqslant 0.4$, the truncation at $m = l + 4$ of the summation in (49) is sufficient, given that the truncation error is less than 1%.

By applying the analytization operation $\mathbf{A}_M$ to the quantity $\widetilde{D}_S^{(l)}(Q^2)$, we finally obtain

$$\widetilde{R}_S^{(l)\mathrm{MFAPT}} = \mathbf{A}_M[D_S^{(l)}] = \\ = 3\,\hat{m}_{(l)}^2 \left[\mathfrak{a}_{\nu_0}^{(l)} + \sum_{n\geqslant 1}^{l} d_n \mathfrak{a}_{n+\nu_0}^{(l)} + \sum_{m\geqslant 1} \Delta_m^{(l)} \mathfrak{a}_{m+\nu_0}^{(l)}\right], \tag{52}$$

where we have used the shorthand notation

$$[a_s(s)^\nu]_{\mathrm{an}} = \mathfrak{a}_\nu^{(l)}(s) \equiv \left(\frac{4}{b_0}\right)^\nu \mathfrak{A}_\nu^{(l)}(s). \tag{53}$$

This expression contains, by means of the coefficients $\Delta_n^{(l)}$ ($e_k^{(l)}$) and the couplings $\mathfrak{a}_{n+\nu_0}^{(l)}$, all renormalization-group terms contributing to this order. On the other hand, the resummed π^2 terms are integral parts of the analytic couplings $\mathfrak{a}_{m+\nu_0}^{(l)}$.

The results for $\widetilde{R}_S(M_H^2)$ as a function of the Higgs mass M_H, calculated with different perturbative approaches in the $\overline{\mathrm{MS}}$ scheme, are shown in Fig. 6. The dashed curve shows the predictions obtained in [27] using standard fixed-order perturbative QCD at the $l = 4$ loop level of the expansion. The solid curve next to it represents the FAPT prediction (cf. (52)), including in the second sum all evolution effects up to $m = l + 4$ and fixing the active flavor number to $N_f = 5$. On the other hand, the contributions of the higher-loop renormalization-group dependent terms are accumulated in the coefficients $\Delta_m^{(l)}$ by means of the parameters γ_i and b_j. Obviously, the standard perturbative QCD approach and FAPT yield similar predictions for this observable, starting with the two-loop running. The reason for the slightly larger FAPT prediction lies in the fact that the coefficients $\mathfrak{a}_\nu$ contain by means of the index ν_0 the resummed contribution of an *infinite* series of π^2 terms (as well as all γ_0 and b_0 terms) that renders them ultimately smaller than the corresponding powers of the standard coupling. Finally, the dotted curve about 8% below the other lines, in both panels

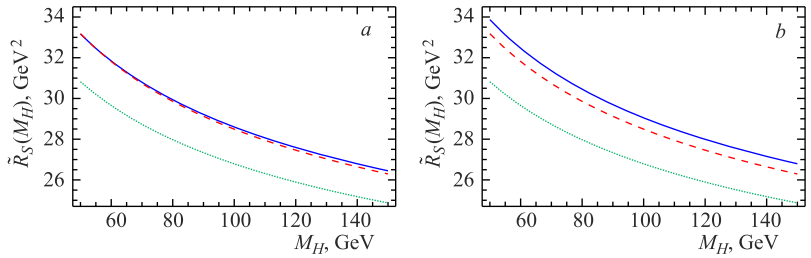

Fig. 6. Predictions for the quantity $\widetilde{R}_S(M_H^2)$ calculated in different perturbative approaches within the $\overline{\rm MS}$ scheme: Standard perturbative QCD [27] at the loop level $l = 4$ (dashed line with $\Lambda_{N_f=5} = 231$ MeV), Broadhurst–Kataev–Maxwell («naive non-Abelianization») including the $O((a_s)^{\nu_0} A_4(a_s))$ terms [28] (dotted line with $\Lambda_{N_f=5} = 111$ MeV), and FAPT [17] obtained from Eq. (52) for $N_f = 5$ (solid line), displayed for two different loop orders: $l = 2$ (*a*, $\Lambda_{N_f=5} = 263$ MeV) and $l = 3$ (*b*, $\Lambda_{N_f=5} = 261$ MeV). The value of $\Lambda_{N_f=5}$ MeV in all cases corresponds to $\mathfrak{A}_1^{(1)}(s = m_Z^2; N_f = 5) = 0.120$

of Fig. 6, illustrates the estimate obtained with the «naive non-Abelianization» and an optimized power-series expansion that makes use of the «contour-improved integration technique» [28].

The above Higgs decay results can be further extended by resumming the whole nonpower series [25], whereas the case of the three-loop running coupling was elaborated in detail in [29]. This way, one may extract more reliable predictions for the width $\Gamma_{H\to b\bar{b}}$ in terms of the Higgs-boson mass M_H. This is indeed possible by employing an appropriate generating function to determine the next two higher expansion coefficients reaching at the truncation level of N^{3}LO an accuracy of the order of 1%, which is even better than the 2% uncertainty involved in the $\overline{m}_b(\overline{m}_b^2)$ estimates. The predictions for the one-loop and the two-loop width are illustrated in Fig. 7 vs. the mass of the Higgs boson for which the Penin–Steinhauser value $\overline{m}_b(\overline{m}_b^2) = (4.35 \pm 0.07)$ GeV [30] was used. Adopting instead the RG-effective b-quark mass $\overline{m}_b(\overline{m}_b^2) = (4.19 \pm 0.05)$ GeV, calculated by Kühn and Steinhauser [31], one obtains results somewhat reduced by about 7%.

Very recently, the ATLAS [33] and the CMS [34] Collaborations from the Large Hadron Collider (LHC) at CERN have reported the discovery of a new particle consistent with the Standrad Model (SM) Higgs boson. The mass measured by CMS is $M_H = 125.3$, while that found by ATLAS is slightly larger (around 126 GeV). A confirmation at the five-standard-deviation level of certainty that this is the Higgs boson is still lacking. Using a mass value of the SM Higgs boson around 125 GeV, we can extract from Fig. 7 the following prediction:

$$\Gamma_{H\to b\bar{b}} = (2.4 \pm 0.15) \text{ MeV}. \tag{54}$$

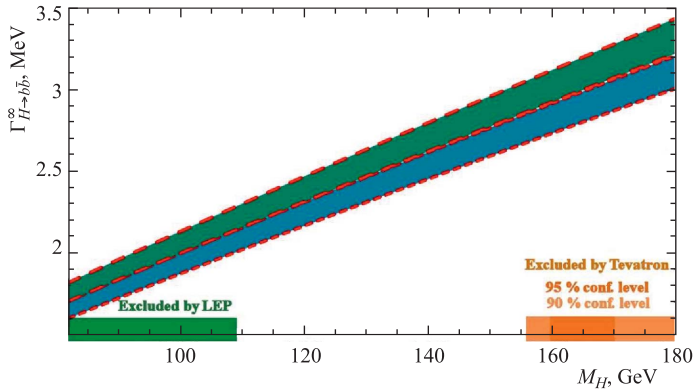

Fig. 7. Predictions for the two-loop width $\Gamma^{\infty}_{H\to b\bar{b}}$ as a function of the Higgs-boson mass M_H using resummed FAPT [25]. The lower strip is obtained by varying the mass in the interval $\hat{m}_{(2)} = (8.22 \pm 0.13)$ GeV according to the Penin–Steinhauser estimate $\overline{m}_b(\overline{m}_b^2) = (4.35 \pm 0.07)$ GeV [30], while the upper strip shows the corresponding one-loop result. The mass window of the Higgs boson that is experimentally accessible is indicated

This estimate covers both the one-loop result (upper strip) as well as the two-loop one (lower strip) and is within the range of $BR(H \to b\bar{b})$ measured very recently by the D0 Collaboration [35].

CONCLUSIONS

FAPT derives from APT and generalizes it both conceptually and technically. Conceptually, it extends the analyticity requirement from the running coupling and its powers to the hadronic amplitude as a whole. Technically, it extends the formalism from integer powers of the coupling to real ones in the spacelike as well as in the timelike region. More recently, progress has been achieved by endowing FAPT with a varying flavor number across heavy-quark thresholds: «flavor-corrected global FAPT» (see [24] for explanations and details). Its numerical realization has quite recently been implemented in the form of the Mathematica package FAPT.m [32]. Yet FAPT is not a complete formalism. We still do not really know how to consider Sudakov gluon resummation within FAPT because under the analytization requirement resummation does not mean exponentiation. This important issue has yet to be understood and developed. Also the application of FAPT to compute power corrections to the spacelike pion's LO electromagnetic form factor and the inclusive Drell–Yan cross section, started in [23], has so far not been exploited beyond the leading power and for other hadronic quantities.

Acknowledgements. I wish to thank A. P. Bakulev and S. V. Mikhailov for a fruitful collaboration and for help in preparing the updated version of this draft. I am also indebted to A. L. Kataev for useful remarks. This work was partially supported by the Heisenberg–Landau Programme (Grant 2009) and the Deutsche Forschungsgemeinschaft under contract 436RUS113/881/0.

REFERENCES

1. *Gross D. J., Wilczek F.* Ultraviolet Behavior of Non-Abelian Gauge Theories // Phys. Rev. Lett. 1973. V. 30. P. 1343–1346.
2. *Politzer H. D.* Reliable Perturbative Results for Strong Interactions // Ibid. P. 1346–1349.
3. *Kataev A. L., Kim V. T.* Uncertainties of QCD Predictions for Higgs Boson Decay into Bottom Quarks at NNLO and Beyond // PoS. 2009. V. ACAT08. P. 004.
4. *Stefanis N. G., Schroers W., Kim H. C.* Pion Form Factors with Improved Infrared Factorization // Phys. Lett. B.1999. V. 449. P. 299;
   Stefanis N. G., Schroers W., Kim H. C. Analytic Coupling and Sudakov Effects in Exclusive Processes: Pion and $\gamma^*\gamma \to \pi^0$ Form Factors // Eur. Phys. J. C. 2000. V. 18. P. 137.
5. *Bakulev A. P. et al.* Pion Form Factor in QCD: From Nonlocal Condensates // Phys. Rev. D. 2004. V. 70. P. 033014.
6. *Cornwall J. M.* Dynamical Mass Generation in Continuum QCD // Phys. Rev. D. 1982. V. 26. P. 1453.
7. *Stefanis N. G.* The Physics of Exclusive Reactions in QCD: Theory and Phenomenology // Eur. Phys. J. C. 1999. V. 7. P. 1–109.
8. *Cornwall J. M., Soni A.* Glueballs as Bound States of Massive Gluons // Phys. Lett. B. 1983. V. 120. P. 431.
9. *Botts J., Sterman G.* Hard Elastic Scattering in QCD: Leading Behavior // Nucl. Phys. B. 1989. V. 325. P. 62.
10. *Li H.-N., Sterman G.* The Perturbative Pion Form Factor with Sudakov Suppression // Nucl. Phys. B. 1992. V. 381. P. 129–140.
11. *Bolz J. et al.* A Critical Analysis of the Proton Form Factor with Sudakov Suppression and Intrinsic Transverse Momentum // Z. Phys. C. 1995. V. 66. P. 267–278.
12. *Stefanis N. G.* Implications of Gluon Radiation Effects and Soft Transverse Momenta for the Nucleon Substructure in QCD // Mod. Phys. Lett. A. 1995. V. 10. P. 1419–1434.
13. *Krasnikov N. V., Pivovarov A. A.* The Influence of the Analytical Continuation Effects on the Value of the QCD Scale Parameter Lambda Extracted from the Data on Charmonium and Upsilon Hadron Decays // Phys. Lett. B. 1982. V. 116. P. 168–170.
14. *Radyushkin A. V.* Optimized Lambda-Parametrization for the QCD Running Coupling Constant in Space-Like and Time-Like Regions // JINR Rapid Commun. 1996. V. 78. P. 96–99; JINR Preprint E2-82-159. Dubna, 1982.

15. *Ball P., Beneke M., Braun V. M.* Resummation of $(\beta_0\alpha_s)^n$ Corrections in QCD: Techniques and Applications to the Tau Hadronic Width and the Heavy Quark Pole Mass // Nucl. Phys. B. 1995. V. 452. P. 563–625.

16. *Beneke M., Jamin M.* α_s and the Tau Hadronic Width: Fixed-Order, Contour-Improved and Higher-Order Perturbation Theory // JHEP. 2008. V. 09. P. 044.

17. *Bakulev A. P., Mikhailov S. V., Stefanis N. G.* Fractional Analytic Perturbation Theory in Minkowski Space and Application to Higgs Boson Decay into a $b\bar{b}$ Pair // Phys. Rev. D. 2007. V. 75. P. 056005.

18. *Shirkov D. V., Solovtsov I. L.* Analytic Model for the QCD Running Coupling with Universal $\bar{\alpha}_s(0)$ Value // Phys. Rev. Lett. 1997. V. 79. P. 1209–1212;
Shirkov D. V., Solovtsov I. L. Ten Years of the Analytic Perturbation Theory in QCD // Theor. Math. Phys. 2007. V. 150. P. 132.

19. *Bogolyubov N. N., Logunov A. A., Shirkov D. V.* The Method of Dispersion Relations and Perturbation Theory // Sov. Phys. JETP. 1960. V. 10. P. 574.

20. *Redmond P. J., Uretsky J. L.* Conjecture Concerning the Properties of Nonrenormalizable Field Theories // Phys. Rev. Lett. 1958. V. 1. P. 147–148.

21. *Bakulev A. P., Karanikas A. I., Stefanis N. G.* Analyticity Properties of Three-Point Functions in QCD Beyond Leading Order // Phys. Rev. D. 2005. V. 72. P. 074015.

22. *Bakulev A. P., Mikhailov S. V., Stefanis N. G.* QCD Analytic Perturbation Theory: From Integer Powers to Any Power of the Running Coupling // Phys. Rev. D. 2005. V. 72. P. 074014; Erratum Ibid. P. 119908.

23. *Karanikas A. I., Stefanis N. G.* Analyticity and Power Corrections in Hard-Scattering Hadronic Functions // Phys. Lett. B. 2001. V. 504. P. 225–234;
Stefanis N. G. Perturbative Logarithms and Power Corrections in QCD Hadronic Functions: A Unifying Approach // Lect. Notes Phys. 2003. V. 616. P. 153.

24. *Bakulev A. P.* Global Fractional Analytic Perturbation Theory in QCD with Selected Applications // Phys. Part. Nucl. 2009. V. 40. P. 715–756.

25. *Bakulev A. P., Mikhailov S. V., Stefanis N. G.* Higher-Order QCD Perturbation Theory in Different Schemes: From FOPT to CIPT to FAPT // JHEP. 2010. V. 1006. P. 085 (1–38).

26. *Gorishnii S. et al.* Corrected Three-Loop QCD Correction to the Correlator of the Quark Scalar Currents and $\Gamma_{\text{tot}}(H^0 \to \text{hadrons})$ // Mod. Phys. Lett. A. 1990. V. 5. P. 2703–2712.

27. *Chetyrkin K. G., Kniehl B. A., Sirlin A.* Estimations of Order α_s^3 and α_s^4 Corrections to Mass-Dependent Observables // Phys. Lett. B. 1997. V. 402. P. 359–366;
Baikov P. A., Chetyrkin K. G., Kühn J. H. Scalar Correlator at O(alpha(s)**4), Higgs Decay into *b* Quarks and Bounds on the Light Quark Masses // Phys. Rev. Lett. 2006. V. 96. P. 012003.

28. *Broadhurst D. J., Kataev A. L., Maxwell C. J.* Renormalons and Multiloop Estimates in Scalar Correlators, Higgs Decay and Quark-Mass Sum Rule // Nucl. Phys. B. 2001. V. 592. P. 247–293.

29. *Bakulev A. P., Potapova I. V.* Resummation Approach in QCD Analytic Perturbation Theory // Nucl. Phys. B (Proc. Suppl.). 2011. V. 219–220. P. 193–200.

30. *Penin A. A., Steinhauser M.* Heavy Quarkonium Spectrum at $O(\alpha_s^5 m_q)$ and Bottom/Top Quark Mass Determination // Phys. Lett. B. 2002. V. 538. P. 335–345.

31. *Kühn J. H., Steinhauser M.* Determination of α_s and Heavy Quark Masses from Recent Measurements of $R(s)$ // Nucl. Phys. B. 2001. V. 619. P. 588–602.

32. *Bakulev A. P., Khandramai V. L.* FAPT: A Mathematica Package for Calculations in QCD Fractional Analytic Perturbation Theory. arXiv:1204.2679 [hep-ph]. 2012.

33. *Aad G. et al. (ATLAS Collab.).* Combined Search for the Standard Model Higgs Boson in pp Collisions at $\sqrt{s} = 7$ TeV with the ATLAS Detector. arXiv:1207.0319 [hep-ex]. 2012.

34. *Chatrchyan S. et al. (CMS Collab.).* Combined Results of Searches for the Standard Model Higgs Boson in pp Collisions at $\sqrt{(s)} = 7$ TeV // Phys. Lett. B. 2012. V. 710. P. 26–48.

35. *Abazov V. M. et al. (D0 Collab.).* Combined Search for the Standard Model Higgs Boson Decaying to $\bar{b}b$ Using the D0 Run II Data Set. arXiv:1207.6631 [hep-ex]. 2012.